SODIUM CHANNEL INACTIVATION IN THE CRAYFISH GIANT AXON

MUST CHANNELS OPEN BEFORE INACTIVATING?

BRUCE P. BEAN, *Department of Radiation Biology and Biophysics and Department of Physiology, University of Rochester Medical Center, Rochester, New York 14642*

ABSTRACT Experiments on sodium channel inactivation kinetics were performed on voltage-clamped crayfish giant axons. The primary goal was to investigate whether channels must open before inactivating. Voltage-clamp artifacts were minimized by the use of low-sodium solutions and full series resistance compensation, and the spatial uniformity of the currents was checked with a closely spaced pair of electrodes used to measure local current densities. For membrane potentials between −40 and +40 mV, sodium currents decay to zero with a single exponential time-course. The time constant for decay is a steep function of membrane potential. The time-course of inactivation measured with the double-pulse method is very similar to the decay of current at the same potential. Steady-state inactivation curves measured with different test pulses are identical. The time-course of double pulse inactivation shows a lag that roughly correlates with the opening of sodium channels, but detailed comparisons with the time course of the prepulse current suggest that it is not strictly necessary for channels to open before inactivating. Measurements of the potential dependence of the integral of sodium conductance are also inconsistent with the simplest cases of models in which channels must open before inactivating.

INTRODUCTION

When a nerve membrane is sufficiently depolarized from its resting potential, the permeability to sodium ions rises and then becomes small again (Hodgkin and Huxley, 1952*a*). A first step in understanding the kinetic mechanism of the sodium channel is to understand the relation of the inactivating phase of the sodium conductance to the initial activating phase. Hodgkin and Huxley (1952*b*) postulated independent activation and inactivation gates, both of which must be open for the sodium channel to conduct ions. However, convincing evidence that activation and inactivation are not independent has recently come from the observation that voltage pulses that produce inactivation also partially immobilize the gating charge associated with activation (Armstrong and Bezanilla, 1977; Meves and Vogel, 1977; Nonner, 1980; Swenson, 1980).

The gating charge immobilization experiments demonstate that the activation process is prevented when the channel is inactivated, but they do not bear on the separate question of whether the state of activation of the channel influences the rate of inactivation. Thus, a

---

Dr. Bean's present address is Department of Physiology, Yale School of Medicine, New Haven, Conn. 06510.

question of current interest is whether sodium channels must first open before inactivating; that is, whether inactivation is strictly coupled to activation.

One reason that the question of activation-inactivation coupling is unsettled is that many of the experiments relevant to the issue have had different results reported in different preparations. For example, Goldman and Schauf (1973) reported that in the *Myxicola* giant axon the rate of inactivation measured with the prepulse method (Hodgkin and Huxley, 1952*a*) was substantially slower than the rate of decay of sodium currents at the same potential. This result would greatly narrow the field of possible inactivation models, since it is inconsistent with a wide range of models, including those in which the rate of inactivation is independent of activation (e.g., the Hodgkin-Huxley model) and those in which inactivation is necessarily coupled to activation. The same result has been reported for lobster giant axons (Oxford and Pooler, 1975), but in the squid giant axon (Hodgkin and Huxley, 1952*a*; Chandler et al., 1965; Bezanilla and Armstrong, 1977; Gillespie and Meves, 1980) and in the frog node (Chiu, 1977; Nonner, 1980) the rates determined by the two methods are nearly identical.

A second observation consistent with only a few types of models involves the measurement of steady-state inactivation as a function of membrane potential. Hoyt (1968) pointed out that certain classes of mathematical models predict that inactivation curves obtained with different test pulses to assay the amount of inactivation could be significantly shifted along the voltage axis relative to one another. This result was obtained experimentally for the *Myxicola* axon (Goldman and Schauf, 1972; Schauf et al., 1976) and for the squid axon (Hoyt and Adelman, 1970; Rudy, cited in Goldman, 1976). But because of the sensitivity of the result to series resistance errors (Goldman and Schauf, 1972), it seems advisable to re-examine this question with particularly close attention to voltage-clamp errors.

The most direct way of testing whether activation influences the rate of inactivation is to observe the time-course of inactivation, determined with the double-pulse method, at short times, while channels are activating. In *Loligo forbesi* axons, Chandler et al. (1965) observed a simple exponential time-course of double pulse inactivation, as if the probability of inactivation is not affected by the opening of the channel. In a number of reports since then, however, inactivation appeared to develop with a lag roughly paralleling the time-course of the opening of channels (Armstrong, 1970; Goldman and Schauf, 1972; Peganov, 1973; Schauf and Davis, 1975; Bezanilla and Armstrong, 1977), as if channels open before inactivating. Gillespie and Meves (1980) re-examined the question in *Loligo forbesi*, again saw little or no lag in inactivation, and suggested that many of the reported instances of lags could have been produced by voltage-clamp artifacts or by inappropriate voltage-pulse protocols.

The primary goal of the work reported here was to investigate the question of activation-inactivation coupling. Because of the possibility that voltage-clamp artifacts have caused some of the inconsistency in the results from other preparations, it seemed especially important to first assess and reduce errors associated with the voltage-clamp method. Series resistance errors were minimized by the use of low sodium concentrations and a new method for more complete series resistance compensation (Sigworth, 1979). Errors arising from longitudinal nonuniformity of potential and current (see Taylor et al., 1960; Cole, 1968) were estimated and reduced by recording localized membrane currents (Cole and Moore, 1960).

With these precautions, double-pulse inactivation matched single-pulse decay, and there was no shift of the inactivation curve with test pulse height. There was, however, a pronounced lag in double-pulse inactivation, which suggests that inactivation becomes faster as channels open. Detailed comparison of the lag with the opening of channels suggested that channels need not necessarily activate completely for inactivation to occur. This conclusion was reinforced by a comparison of sodium conductance integrals at different potentials, intended as a test of strict coupling; the results were inconsistent with the simplest cases of strictly coupled models.

METHODS

Medial giant axons from *Procambarus clarkii* were dissected, cleaned, and voltage clamped by the axial wire technique described by Shrager (1974). Crayfish were from Louisiana and California; there were no apparent systematic differences in the properties of their axons.

Membrane currents were digitized, temporarily stored in an IMSAI 8080 microcomputer (IMS Associates, San Leandro, Calif.), and analyzed with a PDP 8/E minicomputer (Digital Equipment Corp., Maynard, Mass.).

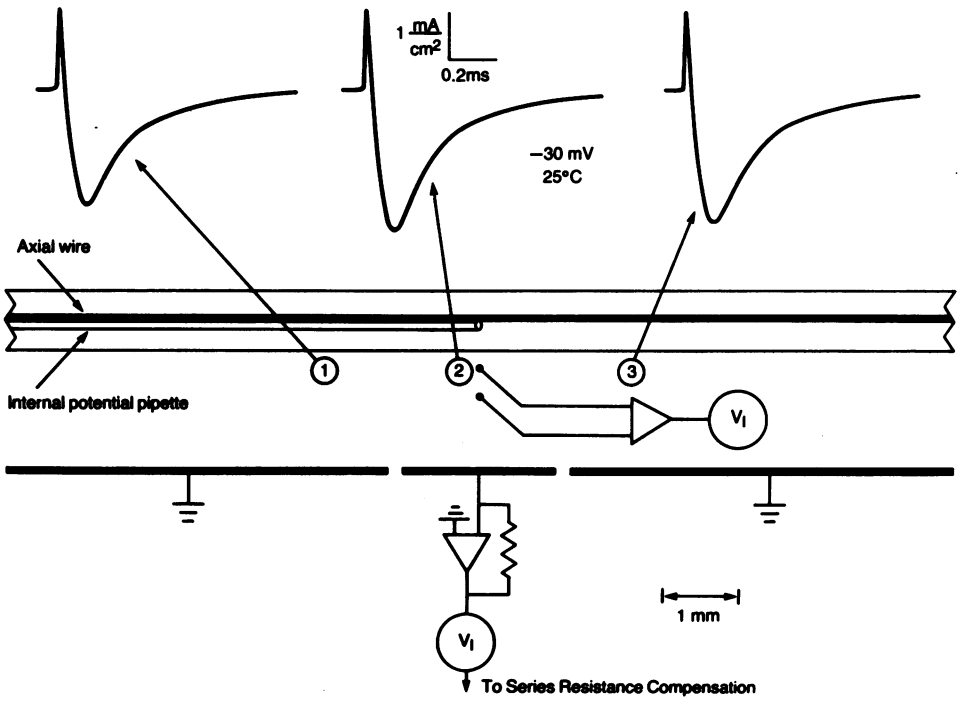

FIGURE 1 Method of current measurement. Not drawn to scale in the vertical direction; a typical axon diameter is 200 μm, and the external platinum plate ground electrodes were usually ~3 mm from the axon. The currents shown were recorded at three positions: with the differential electrode opposite the control point (*1*), 2 mm to the left (*2*), and 2 mm to the right (*3*). The nearer wire of the electrode was ~700 μm from the axon. Current density was calculated by comparing current signals recorded with the differential electrode with those from the central plate; in this axon, the calibrating factor was 1 mA/cm² for 0.73 mV between the wires in the differential electrode. Full Na, Full K, 1 mM 4-AP, 2.5°C.

Current Measurement

To clamp the membrane potential, current was passed with the internal axial wire to an external electrode consisting of three platinized platinum plates of lengths 5, 2, and 5 mm, as shown in Fig. 1. Membrane current density was measured by recording current density in the external solution as the potential drop between a pair of platinized platinum wire electrodes separated by 180 μm and oriented perpendicular to the axon (Fig. 1), a technique devised by Cole and Moore (1960; see also Cole, 1968) to permit measurement of relatively localized membrane current density. The wires had diameters of 25 μm and were insulated except for the final 170 μm. The nearer wire was usually within 80 μm of the axon when the electrode pair was in its final position at the "control point" opposite the tip of the internal potential pipette. The signal from the differential electrode was amplified and high-pass filtered at 0.06 Hz and low-pass filtered at 14 kHz before being digitized.

The spatial resolution of the electrode pair was calibrated as shown in Fig. 2. A pipette "point" current source in the nerve chamber simulated a small piece of axon membrane, and the electrode pair was moved parallel to the axis of the pipette. The size of the signal recorded at various positions relative to that recorded opposite the mouth of the pipette ($x = 0$) is shown in Fig. 2. The solid line in Fig. 2 gives the values expected if the field due to the source falls off as $1/r^{3/2}$ in the plane parallel to the floor of the chamber. This approximation is reasonably good, judged both by the fit to the data in Fig. 2 and by direct measurement of potentials in the chamber. Knowing how the current from a small source will spread in the chamber, together with the geometry of the axon and electrode pair, permits an estimation of the contribution of parts of the axon membrane at various distances to the total recorded current signal.

Series Resistance Compensation

In order to increase the amount of series resistance compensation (Hodgkin et al., 1952) that could be employed without inducing oscillations in the voltage-clamp system, the current signal was low-pass

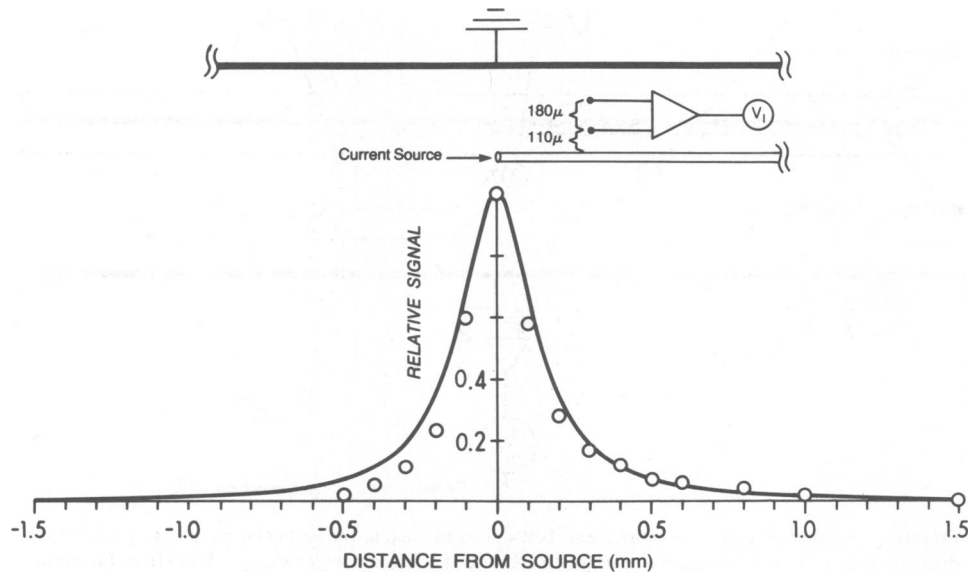

FIGURE 2 Spatial resolution of the differential electrode. The pipette current source was in the chamber in the position normally occupied by the axon, ~3 mm from the ground electrode and about 100 μm above the floor of the chamber. Points give the recorded voltage signals normalized with respect to that recorded opposite the mouth of the pipette. The solid line is drawn according to $y = 1/(x^2 + a^2)^{1/4} - 1/[x^2 + (a + b)^2]^{1/4}$, with a, distance of nearer wire from source, = 110 μm and b, separation of wires, = 180 μm.

filtered at 12 kHz before being fed back into the voltage-clamp amplifier (Sigworth, 1979). The current signal from the central plate of the external current electrode was used for series resistance compensation since the signal from the differential electrode pair had an unstable DC component. Compensation for 10–13 ohm-cm^2 was used. The series resistance measured from the time constant of the capacitative transient, in an axon in which the membrane capacitance was independently measured, was 11 ohm-cm^2. The effective series resistance was also estimated in a number of axons with deliberate undercompensation by examining the changes in current kinetics produced by changes in current sizes. For example, in an axon in which compensation for 3 ohm-cm^2 was used, sodium current sizes were reduced by successive reductions of external sodium from 210 to 105 to 52 mM; the changes in the time-course of decay of currents in the range −40 to 0 mV could be well fit by assuming a residual uncompensated series resistance of 6 ohm-cm^2. In other experiments, current sizes were changed by changes in the holding potential; these also led to estimates of about 10 ohm-cm^2 for the total series resistance. Thus, the compensation for 10–13 ohm-cm^2 was probably close to being complete in each axon.

Except for the currents shown in Fig. 1 and the inset to Fig. 3, all the experiments reported in this paper were performed with external sodium concentrations of ≤52 mM, and peak inward currents were generally <1 mA/cm^2. It is unlikely that series resistance errors were ever >4–5 mV, and they were probably usually much less.

Solutions

The dissection and electrode insertion were performed in van Harreveld's (1936) solution. Sodium currents were usually recorded in low-sodium, low-potassium solutions containing 1 mM 4-aminopyridine (4-AP) to block potassium currents. The solution used in most experiments (1/4 Na, 1/2 K, 1 mM 4-AP) was a modification of van Harreveld's solution containing 52 mM NaCl, 2.7 mM KCl, 13.5 mM

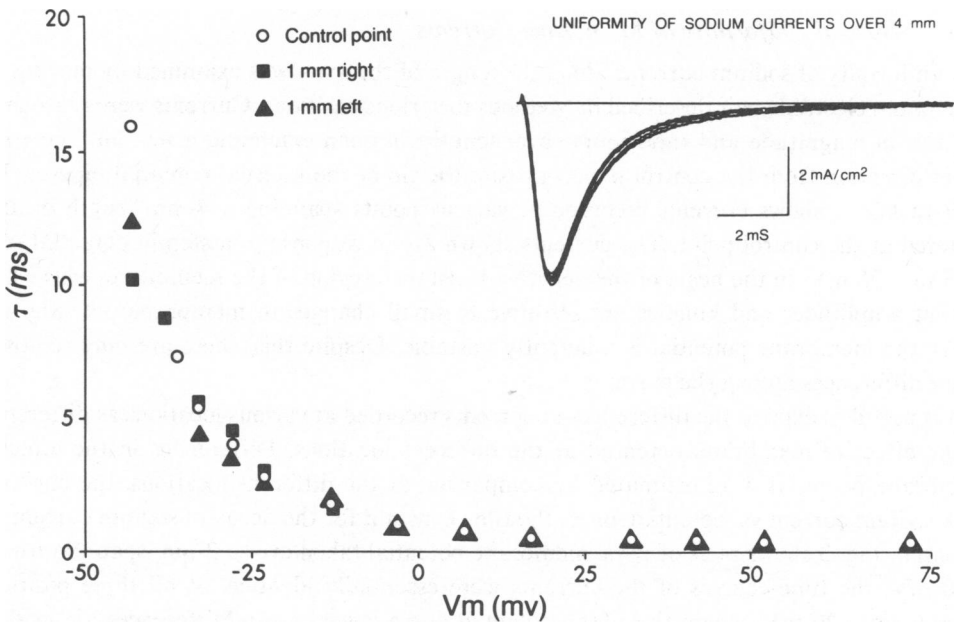

FIGURE 3 Decay time constant vs. membrane potential at three positions. The nearer wire was 100–200 μm from the axon. 1/10 Na, 2/5 K, 1 mM 4-AP. Holding potential −83 mV. 4.2–4.4°C. *Inset:* Spatial uniformity of currents in response to a depolarization from −75 to −25 mV. Currents were recorded at five positions: opposite the control point, 1 mm right, 2 mm right, 1 mm left, and 2 mm left. The nearer wire of the electrode was 300–400 μm from the axon. Leak and capacitative currents were corrected for by adding the current from a hyperpolarizing pulse. Full Na, Full K, 1 mM 4-AP, 1.8°C.

$CaCl_2$, 2.6 mM $MgCl_2$, 1 mM 4-AP, 2.3 mM Hepes buffer, with tetramethylammonium chloride (TMA) added to yield 433–438 mosmol. The solutions named with other fractional sodium or potassium concentrations were the same except for greater or less substitution by TMA. Solutions were adjusted to pH 7.5–7.6.

Isolation of Sodium Currents

Potassium currents were completely blocked by 1 mM 4-AP for depolarizations negative to about −10 mV; there was some relief of block at more positive potentials (Yeh et al., 1976), but sodium current inactivation was virtually complete before the small, slow residual potassium currents became appreciable (see Fig. 5). Sodium currents appeared to be unaffected by 4-AP: the rise and early decay of sodium currents were unchanged during the application of 4-AP; moreover, sodium currents obtained without 4-AP, with TTX subtraction, were quantitatively similar in every way to currents obtained with 4-AP.

In most experiments, leak and linear capacitative currents were corrected for by addition or subtraction of suitably scaled currents from hyperpolarizations or subthreshold depolarizations.

In some experiments, especially for large depolarizations, leak, capacitative, and residual potassium currents were obtained by a double-pulse procedure in which the test pulse was preceded by a conditioning prepulse sufficient to completely inactivate sodium current. This procedure is illustrated in Fig. 5. The prepulse was separated from the test pulse by a short return to rest, so that the capacitative current was the same in the test pulse with the prepulse as without the prepulse. Except for a small component of gating current, this "prepulse subtraction" technique gave results identical to those from a TTX-subtraction procedure in axons in which both were used.

RESULTS

Spatial Uniformity of Membrane Currents

The uniformity of sodium currents along the length of the axon was examined by moving the differential electrode pair described in Methods to various positions. Currents were reasonably uniform in magnitude and time-course over lengths of axon extending a few millimeters in either direction from the control point opposite the tip of the internal potential pipette. The inset to Fig. 3 shows currents recorded at various points spanning a 4-mm length of axon centered at the control point. The currents shown are in response to a step in potential from −75 to −25 mV, in the heart of the negative-resistance region of the membrane, where both current amplitudes and kinetics are sensitive to small changes in membrane potential and where the membrane potential is inherently unstable. Despite this, there are only relatively minor differences among the currents.

It is useful to express the differences in currents recorded at various locations as differences in the effective membrane potential at the different locations. Differences in the effective membrane potential were estimated by comparing, at the different locations, the curves of peak sodium current vs. potential; or τ_h, the time constant for the decay of sodium current, vs. potential. Fig. 3 shows plots of τ_h vs. membrane potential taken over a 2-mm span. Positive to −20 mV, the time-courses of the currents were essentially identical at all three positions; negative to −20 mV, where the τ_h-vs.- potential curve is very steep, differences are evident. The points from currents recorded 1 mm left are shifted by ~3 mV relative to those at the control point; this is seen most clearly in the −35 to −20-mV range. The points from currents recorded 1 mm right are very similar to those from the control point; the effective shift at any potential is <1 mV. Considering the whole span, then, for any given voltage pulse, the currents

over the 2-mm length originate from areas of membrane differing in potential by 4 mV or less.

The uniformity of effective membrane potentials determined by means of the shift in the, τ_h-vs.-membrane-potential curve, for five axons is shown in Table I. Usually the shift was determined in the region around -25 mV; here the curve was sufficiently steep to be sensitive, while the currents were big enough for accurate determinations of τ_h. These were typical axons which were "good" in the sense that they had stable resting potentials in the range -72 to -76 mV in van Harreveld's solution at 3–4°C. A few axons had low or unstable resting potentials (and were not used for experiments); most had been seen to be damaged during entry of the piggy-back electrode. These axons often had spectacularly nonuniform currents, which lends confidence to the resolving power of the differential electrode.

Knowing approximately the magnitude of variations in potential along the length of the axon, and knowing the resolving power of the electrode, as shown in Fig. 2, allows one to estimate how much variability in membrane potential there will be in the areas of membrane that contribute significant amounts of current density to the differential electrode when it is in its final position opposite the control point. If the electric field due to a current source spreads as $1/r^{3/2}$, as in the solid line in Fig. 2, then for the differential electrode with spacing 180 μm, with the nearer wire 70 μm from the axon, for an axon diameter of 200 μm, numerical approximations lead to the result that 75% of the signal would originate from about a 0.7-mm length of axon centered at the control point. 90% of the signal would originate from about a 1.5-mm length. (This assumes equal membrane current densities along the axon's length.) Therefore, the estimations given in Table 1 of membrane potential uniformity over a 2-mm span translate fairly directly into estimations of the potential uniformity represented by the signal recorded at the control point by the differential electrode. Of course, the largest contributions come from the nearest portions of membrane, which are closest to the command potential.

The most common pattern of deviation from strict uniformity was that seen in Fig. 3: the effective membrane potentials 1 mm right were very similar to those at the control point, but the membrane 1 mm left was effectively more depolarized by 2–4 mV by the same pulse. This pattern of deviation was undoubtedly mainly due to the fact that the axial wire of the

TABLE I
SPATIAL UNIFORMITY OF EFFECTIVE MEMBRANE POTENTIALS

Axon	External sodium concentration	Potential variation	
		In 2-mm length	In 4-mm length
		(mV)	
1	Full	3	5
2	Full	4	5
3	1/4	5	7
4	1/4	4	6
5	1/4	3	5
6	1/4	6	
7	1/10	4	

piggy-back electrode was fastened to the potential pipette by a dab of laquer about 400 μm long, located ~1 mm behind the tip of the pipette. The current density delivered by the axial wire was, therefore, not at all homogeneous in this region, and some nonuniformity in membrane potential is to be expected.

A procedure that was not optimal for recording currents from the smallest possible area of membrane was the use of ground plates on only one side of the axon. In several experiments, two plates were used, one on either side of the axon. The spatial uniformity was not significantly better with two plates, and the small increase in the effective resolving power of the electrode with this arrangement, owing to less relative contribution by the areas of membrane on the far side of the axon, did not compensate for the smaller total signal and consequent decrease of the signal-to-noise ratio.

Decay of Sodium Conductance

Fig. 4 shows the time-course of sodium conductance at three membrane potentials in a single axon. The initial downward deflection is due to gating current; leak and capacitative current were corrected for by adding currents from hyperpolarizations. The falling phases of the conductances have been fit with exponentials declining to zero; the fit is excellent at all three potentials. The exponentials were fit between the times at which conductance had declined to 75 and 30% of its peak value, in order to emphasize any deviation from a single exponential at longer times.

Sodium currents decayed exponentially to zero at most potentials in all axons. In many

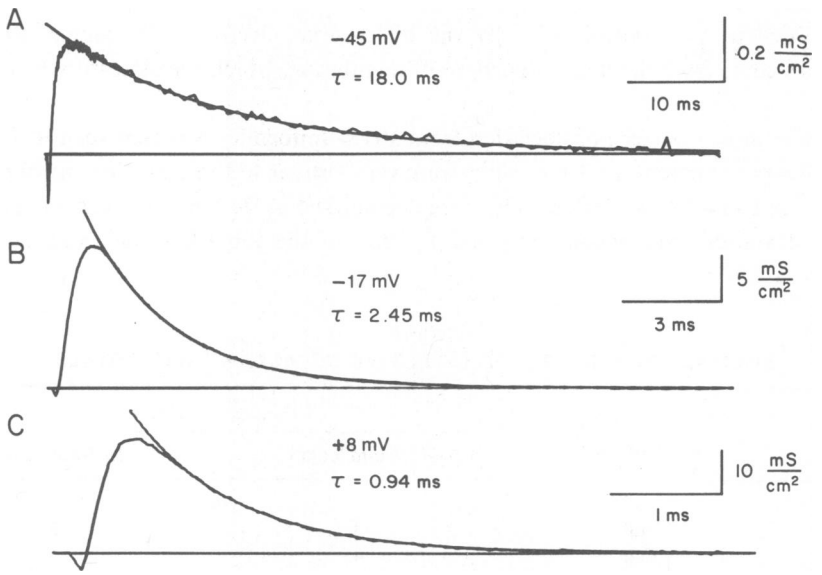

FIGURE 4 Exponential decay of sodium conductance. Currents have been divided by the driving force (membrane potential–reversal potential) to give conductances. Leak and capacitative currents were corrected for by adding currents from hyperpolarizations. *A*, Signal-averaged sum of 16 depolarizing and 16 hyperpolarizing sweeps. Small spike near the end of the record corresponds to the termination of the depolarization. *B–C*, Sums of single sweeps, one depolarizing and one hyperpolarizing. ¼ Na, ½ K, 1 mM 4-AP, 3.5°C.

axons, currents between −35 and −30 mV exhibited small deviations from exponential decay. These deviations probably represent small spatial variations in membrane potential, since they were lacking in axons with the best spatial uniformity characteristics.

A second region of membrane potential where the fit to a single exponential was generally not excellent is for large depolarizations, to potentials greater than ~+40 mV. There was a second small, slower component to the decay of currents at these potentials; this is shown in Fig. 5 for a depolarization to +86 mV. In this range of potentials, the deviation from single exponential decay probably represents a genuine property of the sodium channel kinetics. It is not an artifact of the use of 4-AP, since currents obtained by TTX subtraction looked exactly the same.

In most axons, sodium currents inactivated completely even for the smallest depolarizations for which sodium current could be seen with signal averaging, at potentials near −45 mV (see, for example, Fig. 7). In a few axons, however, sodium currents in this region appeared to decay to a nonzero asymptote. The asymptote was always <10% of the peak value; the decay to the asymptote was exponential.

Double-Pulse Measurement of Inactivation

Fig. 6 compares the time-course of inactivation determined by the double-pulse method with the decay of current at the same potential. The points representing peak test pulse currents in a double-pulse procedure (see inset) are plotted superimposed on the record of sodium current at the prepulse potential. The ordinates have been scaled so that the two curves match when the single pulse current has decayed to about half of its peak value. At both potentials examined in this axon, the time-courses of inactivation reported by the two methods are very similar over the times at which they may be compared. Of particular interest for kinetic models of sodium channels are the kinetics of inactivation for small depolarizations; it is in this

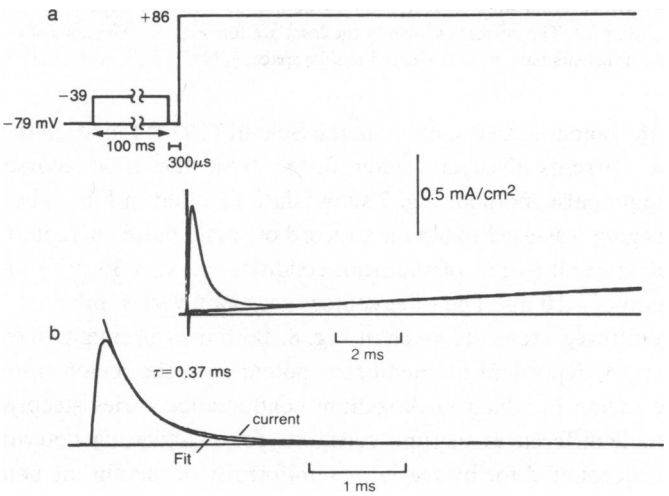

FIGURE 5 Sodium current at +86 mV. (*a*) Pulse protocol and currents. The test pulse to +86 mV was preceded by a 100-ms prepulse to −39 mV in order to inactivate sodium current; the resultant current was subtracted from the test pulse current with no prepulse to yield sodium current. (*b*) Sodium current obtained in this way superimposed with an exponential fit to the current; fit was between 75 and 25% of the peak current. ¼ Na, ½ K, 1 mM 4-AP, 3.9°C.

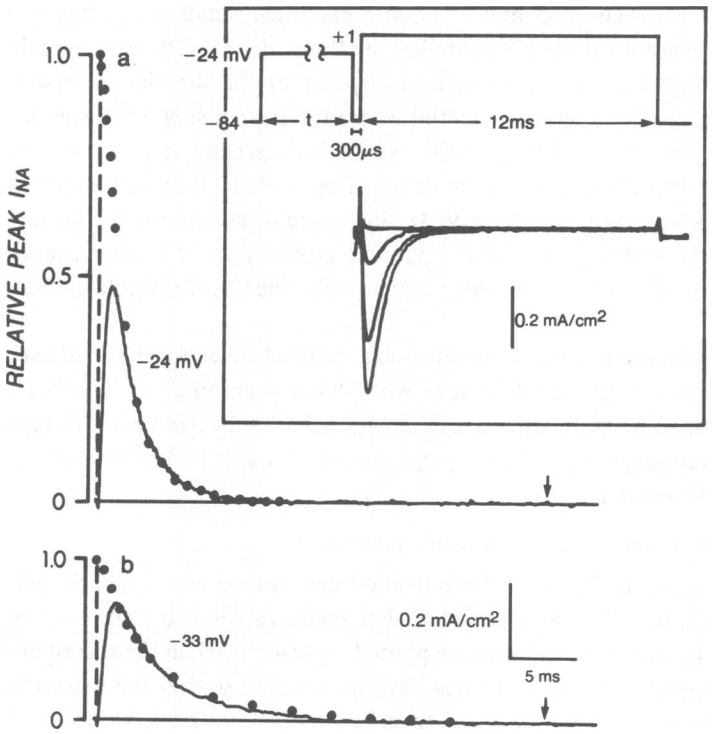

FIGURE 6 Comparison of double-pulse inactivation with sodium current decay. The normalized double-pulse points have been scaled to match the currents when the decay of the currents is about 50% complete. The currents are inward and have been plotted with inward current positive for convenient comparison with the double-pulse points. Dashed lines indicate start of the depolarization; arrows indicate termination. Leak and capacitive currents were corrected for by adding currents for hyperpolarizations. *Inset*: The pulse pattern used in (*a*). The currents shown in the inset are for prepulse durations of 0, 1, 3, and 12 ms. The capacitative transients have been truncated to save space. ¼ Na, ½ K, 1 mM 4-AP, 3.2–3.6°C.

region of membrane potential that Goldman and Schauf (1973) found, in the *Myxicola* axon, that single pulse currents decayed much faster than the time course of inactivation determined by the prepulse method. Fig. 7 shows data like that in Fig. 6, but from an axon in which signal averaging was used to obtain a record of single pulse current at −42 mV, where peak conductance is small (~1/7 of the peak conductance at +36 mV) and decays slowly, with a time constant of ~10 ms. The time-courses are again very similar.

Pooled data from three axons are given in Fig. 8. Both measurements show that the rate of inactivation is sharply dependent on membrane potential in the region from −50 to 15 mV, which is also the region in which peak sodium conductance varies steeply with membrane potential. The small differences in time constants for inactivation determined by the two procedures can be accounted for by spatial nonuniformity of membrane potential amounting to a few mV.

Steady-state Inactivation Determined with Different Test Pulses

There are a number of reports that the steady-state inactivation curve shifts with test pulse height, as long as at least one of the test pulses is on the negative limb of the peak

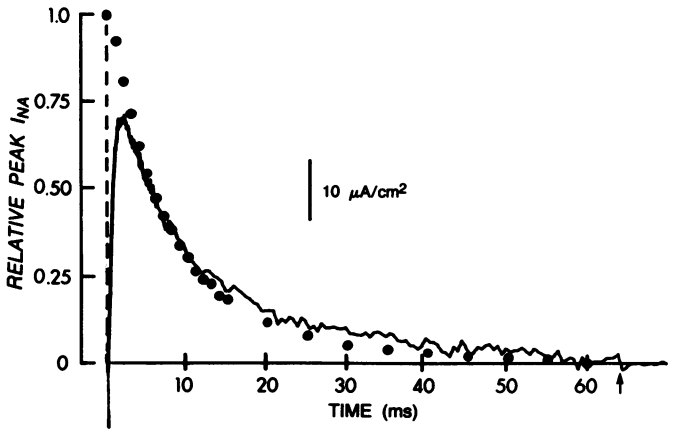

FIGURE 7 Time-courses of double-pulse inactivation and sodium current decay at −42 mV. Current is the signal-averaged sum of 16 depolarizing and 16 hyperpolarizing pulses. Double-pulse points are scaled to match when the current has decayed about halfway. Dashed line indicates start of pulse; arrow indicates end. ¼ Na, ½ K, 1 mM 4-AP, 3.5–3.6°C.

current-voltage curve (Hoyt and Adelman, 1970; Goldman and Schauf, 1972; Schauf et al., 1976). There are no reports to the contrary; Chandler and Meves (1965) observed identical curves with different test pulses, but both test pulses were on the positive limb of the current-voltage curve.

In Fig. 9 are shown the results of an experiment designed to test for this effect in the crayfish axon. Prepulses of 100 ms were followed by test pulses to −34 or +51 mV, and the resulting steady-state inactivation curves obtained with the two test pulse potentials are compared. In the experiment in Fig. 9, the prepulse and test pulse were separated by a 300-μs

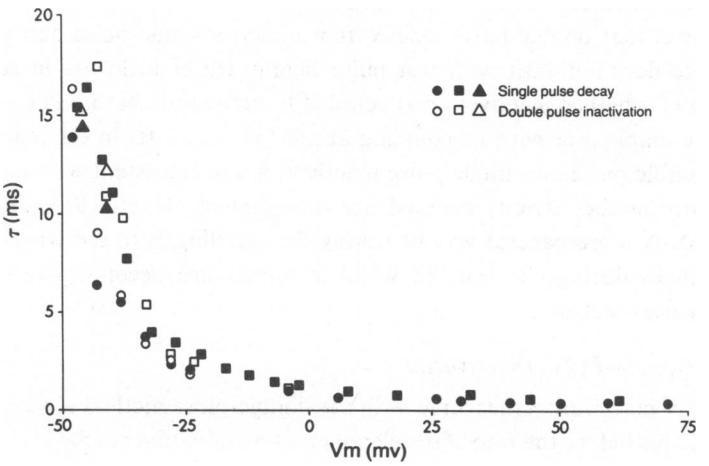

FIGURE 8 Collected double-pulse inactivation and current decay data for three axons. Each symbol represents a different axon. Time constants were obtained from exponental fits to the decay phases of the currents and to the double-pulse inactivation curves after the initial lag. ¼ Na, ½ K, 1 mM 4-AP for all axons. Experiments performed at 3.2–3.6°C.

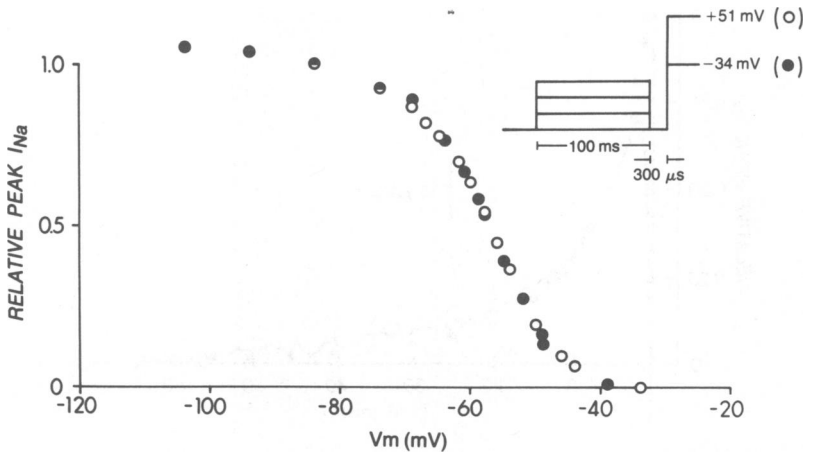

FIGURE 9 Absence of shift in steady-state activation curve with test-pulse height. Steady-state inactivation curves were obtained by giving a 100-ms prepulse to a variable potential, returning to the holding potential for 300 μs, and stepping to the test-pulse potential. The peak currents during the test pulses are plotted as a function of the prepulse potential, normalized to the value for a step from −84 mV, the holding potential. The data points for −94 and −104 mV for the −34-mV test pulse show that there was virtually no inactivation at −84 mV; peak current was about 5% increased by the 100-ms prepulse to −104 mV, and much of this may have been due to removal of slow inactivation. Peak conductance at −34 mV was 0.19 of that at +51 mV. ¼ Na, ½ K, 1 mM 4-AP, 3.3–3.5°C.

return to the holding potential, so that the capacitative currents would be the same in all test pulses, and so could be subtracted more easily. The curves obtained with the two test pulses are identical. In this axon, the peak conductance at −34 mV was about one-fifth of that at +51 mV. In the *Myxicola* axon the steady-state inactivation curve shifts 5.8 mV for a twofold increase in peak sodium conductance (Goldman and Schauf, 1972), so that if such a shift existed in the crayfish axon it would have been detected.

The observations that double-pulse inactivation matches single-pulse decay and that the inactivation curve does not shift with test pulse height are of little use in considering the general question of whether inactivation is coupled to activation: both results are consistent either with strict coupling or with no coupling at all. In fact, shifts in the inactivation curve and dissimilar double pulse and single pulse inactivation are consistent with only a few types of models that are neither strictly coupled nor independent (Hoyt, 1968; Goldman, 1975; Jakobsson, 1976). A more general way of testing for coupling is to see whether the rate of inactivation changes during the time in which channels are becoming activated. This is considered in the next section.

Lag in Double-Pulse Inactivation

The time-course of inactivation measured with the double-pulse method always showed a lag, a delay of 0.1–0.2 ms before the rate of development of inactivation reached its maximum. An example of the lag in double-pulse inactivation for a prepulse to −18 mV is shown in Fig. 10. The peak test-pulse current amplitude decays exponentially for times greater than ~1.5 ms, but at early times the decay is much slower.

The peak test-pulse current in a double-pulse experiment will be proportional to the fraction

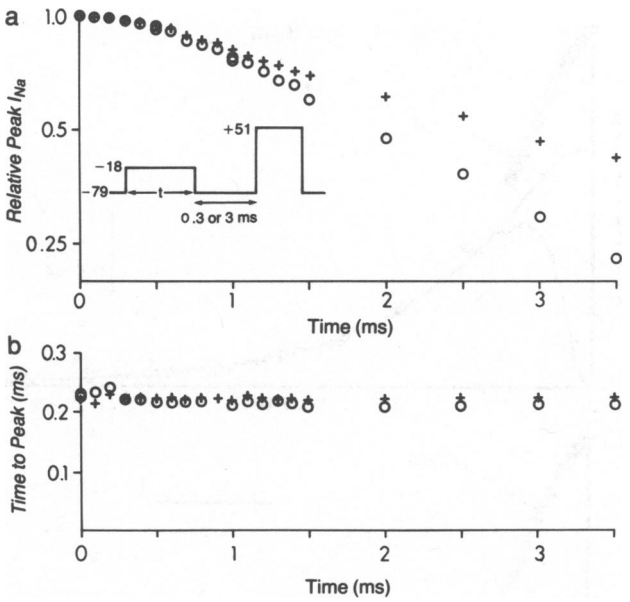

FIGURE 10 Lag in double-pulse inactivation: effect of recovery interval. (*a*) Double-pulse inactivation at −18 mV with recovery interval of 0.3 (○) or 3 (+) ms. (*b*) Time to peak test-pulse current as a function of prepulse duration, for the same currents as in (*a*). ¼ Na, ½ K, 1 mM 4-AP, 3.5°C. Holding potential −79mV.

of noninactivated channels only if the noninactivated fraction begins in the same state or distribution of states with a prepulse as without a prepulse. If the repolarization interval after the prepulse is too short, at the start of the test pulse some channels will be in the open state or in intermediate states between the resting state and the open state; the test-pulse current will reach a peak earlier, and a larger fraction of the noninactivated channels will be open at the peak than for a test-pulse current with no prepulse. This effect can produce an apparent lag even in kinetic models in which inactivation is first-order. The Hodgkin-Huxley model can show significant lags if the test pulse follows the prepulse directly (Kniffki, et al., 1978), and Gillespie and Meves (1980) have demonstrated the effect experimentally in the squid axon.

This effect is not the cause of the lag seen with double-pulse experiments in the crayfish axon. At about −80 mV (2°C), the usual level for the holding and repolarization potential in these experiments, tail currents that follow the interruption of a depolarization decay to ~5% of their initial value in 300 μs, the usual repolarization interval, as if repriming of the channels is nearly complete. With test pulses to ~0 mV, the test current time-to-peak decreases only slightly with prepulses (for example, the largest decrease was <3% in the experiment shown in Fig. 11) and the decreases are not nearly sufficient to account for the lags seen. For more positive test pulses, changes in test current time to peak are even smaller, although the lag in inactivation is no less evident (Fig. 10). Fig. 10 also shows the effect of increasing the repolarization interval to 3 ms: although this is long enough for substantial recovery from inactivation to occur, there is virtually no effect on the time-course of the lag. Thus, the lag is not caused by an insufficient recovery interval between the pulses.

Large series resistance errors can give rise to artifactual sigmoidal time-courses for

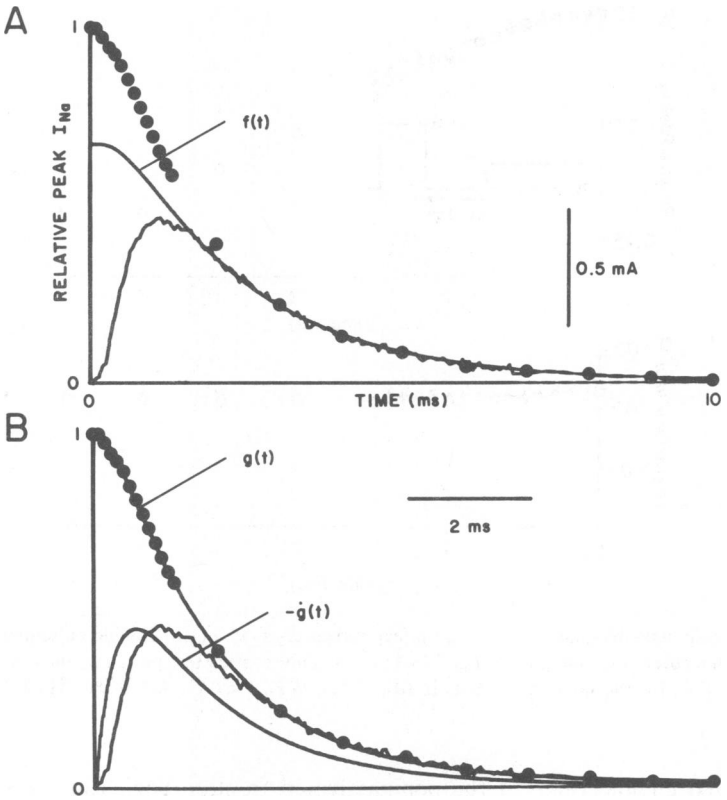

FIGURE 11 Lag in double-pulse inactivation: comparison with prepulse current. *A*, The time-course of double-pulse inactivation is compared with current decay at the prepulse potential of −24 mV; same experiment as Fig. 5*a*. The curve labeled $f(t)$ was calculated as

$$f(t) = 1 - \left[\int_0^t I_{Na} \cdot dt \Big/ \int_0^{t_0} I_{Na} \cdot dt\right],$$

with t_0 = 64 ms. Leak and linear capacitative currents were subtracted by subtracting scaled currents for a subthreshold depolarization to −54 mV; gating current was subtracted by repeating the same procedure in 100 nm TTX and subtracting the result. This procedure took account of a slight increase of leak current which occurred before TTX was applied. *B*, Same data; $g(t)$ is an empirical fit to the double-pulse inactivation points; the negative of its time derivative is plotted scaled to match the peak current height. ¼ Na, ½ K, 1 mM 4-AP, 3.0–3.5°C.

double-pulse inactivation (Gillespie and Meves, 1980). It is very unlikely that such artifacts are responsible for the lags seen in the crayfish axon. As described in Methods, the series resistance compensation was, in principle, complete, and all experiments were done with low external sodium concentrations to reduce current sizes. Lags with typical time-courses were seen in an experiment performed with 21 mM sodium, with peak currents of ~0.2 mA/cm^2. Even large series resistance errors would not be expected to give lags of the sort shown in Figs. 10 and 11, but should result in time courses of inactivation which begin and end with the "true" time constant of inactivation, and which decay more rapidly in the midregion, owing to the extra depolarization caused by the voltage drop across the series resistance when sizeable

current is flowing. In contrast, the data generally show a very good approximation to simple exponential decay after the lag. For the potentials at which the lag is most dramatic (−20 to +5 mV), a time constant fit to the first few hundred microseconds of double-pulse inactivation is at least a factor of four or five greater than the time constant fit to the last tenth or so of the decay, although the prepulse current is very small at both times and series resistance errors would be minimal. It is not obvious how to explain the lag in double-pulse inactivation except as a genuine property of the sodium channels.

How accurately does the development of double-pulse inactivation correlate with the sodium conductance during the prepulse? This comparison is an important test for coupling between activation and inactivation. For the simplest strictly coupled models, in which channels must open before inactivating, the rate of development of inactivation would be proportional to the number of channels able to undergo inactivation, that is, to the number of open channels, and to sodium conductance. Chandler et al. (1965) performed a double-pulse experiment designed to test such a mechanism; their data showed no lag and was better fit by an exponential decay than by a curve drawn on the assumption that the rate of inactivation was proportional to sodium current during the prepulse. The result of this same experiment performed in the crayfish axon is shown in Fig. 11 *A*: the curve labeled $f(t)$ was calculated on the assumption that the rate of inactivation is proportional to the sodium current. Although both $f(t)$ and the time-course of double-pulse inactivation show an initial lag and then exponential decay, they are not identical. The main difference is that the double-pulse data points show less of a lag at early times; that is, there is more inactivation occurring at early times than would be expected if the rate of inactivation were proportional to the sodium current.

A direct comparison of the rate of inactivation with sodium current is shown for the same data in Fig. 11 *B*. A smooth curve, the sum of two exponentials and a constant, was fit to the double-pulse inactivation points. The derivative of this curve, which gives the rate of inactivation, is plotted on the same time scale as the sodium current. In this example, and in other cases at different potentials in different axons, the rate of inactivation is not proportional to sodium current; it rises faster and reaches a peak earlier. Thus, it is not necessary for channels to open before inactivating. This conclusion is reinforced by the results in the next section.

Testing Simple Coupled Models

The simplest model for strictly coupled inactivation kinetics, in which channels must open before inactivating, is

$$\text{Closed} \rightarrow \rightarrow \rightarrow \text{Open} \xrightarrow{K} \text{Inactivated} \qquad \text{(Scheme 1)}$$

for potentials at which inactivation is complete; for potentials at which inactivation is incomplete, there would have to be a significant rate constant for the Inactivated → Open transition as well. Bezanilla and Armstrong (1977) have shown that models of this type with the rate constant K being voltage-independent can account for the main features of inactivation.

Scheme 1 makes predictions about the form of sodium currents that can be tested fairly simply. In this model, the rate of inactivation is given by the fraction of the channels in the open state multiplied by the rate constant K. The results of the previous section suggest that

the rate of inactivation is not strictly proportional to the number of open channels and would be inconsistent with Scheme 1. There is another, similar, calculation that rules out the simplest case of Scheme 1, with K being voltage independent. This approach is based on the observation that this model predicts that at all membrane potentials where inactivation is complete (positive to −40 in the crayfish axon, Fig. 9), the integral of the sodium conductance during a depolarizing pulse will be a constant. The rate of inactivation is proportional to the fraction of open channels:

$$\mathrm{d[Inactivated]}/\mathrm{d}t = [\mathrm{Open}] \times K.$$

Integrating from 0 to ∞, since all the channels become inactivated,

$$1 = \int_0^\infty \mathrm{d[Inactivated]} = \int_0^\infty K \times [\mathrm{Open}]\, \mathrm{d}t$$

$$= K \times \int_0^\infty [\mathrm{Open}]\, \mathrm{d}t, \qquad \text{(Expression 1)}$$

and if K is not voltage-dependent, the integral ought to be the same at each membrane potential. This prediction is independent of the details of the activation steps.

The experimental results are shown in Fig. 12. It is clear that the integral of sodium conductance is not independent of membrane potential: the integral is at a maximum in the region −10 to −20 mV, and is much smaller at more negative membrane potentials and is also smaller at more positive potentials. The smaller values at negative potentials are not simply due to the time constants for decay being so long that the integral was not calculated for long enough times; the time constants for decay in the axons shown in Fig. 12 were about 10 ms near −40 mV, and with the 64-ms pulse duration used in one of the axons, the current had decayed to <1% of its peak value. The integrals of conductance plotted in Fig. 12 were calculated on the basis of an ohmic conductance,

$$G_{\mathrm{Na}} = I_{\mathrm{Na}}/(V_{\mathrm{m}} - V_{\mathrm{Rev}}),$$

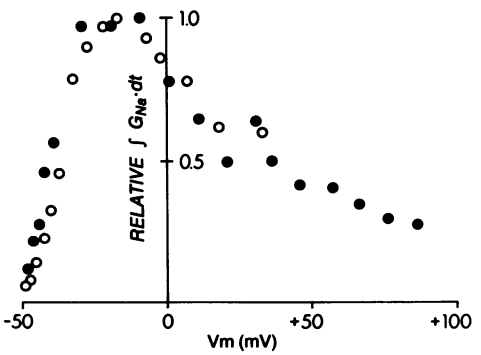

FIGURE 12 Dependence of integrals of sodium conductance on membrane potential. Data from two axons; the integrals in each axon were normalized with respect to the largest value. Open symbols: ¼ Na, ½ K, 1 mM 4-AP, 3.5°C. Leak and capacitative current corrected for by hyperpolarizing pulse currents. Filled symbols: ¼ Na, ½ K, 1 mM-4AP, 3.6°C. Leak and capacitative current corrected for by prepulse-inactivation method.

where V_{Rev} is the reversal potential. The instantaneous current-voltage curve was determined for the sodium channels in one of the axons in Fig. 12, and was linear from −30 to +60 mV.

The nonmonotonic dependence of integrated sodium conductance on membrane potential in Fig. 12 is inconsistent with any version of Scheme 1 with an inactivation rate constant showing a monotonic dependence on membrane potential. Since it is unreasonable for a single rate constant to be a nonmonotonic function of membrane potential, the results in Fig. 12 rule out all physically reasonable cases of Scheme 1. The most straightforward interpretation of the data from −50 to −10 mV would be that at more negative potentials, where activation is incomplete, many channels inactivate without first opening. The decrease of the integrated conductance positive to 0 mV, where activation is complete, is most simply interpreted as a voltage-dependence of the rate constant governing inactivation of open channels.

DISCUSSION

Comparison of Inactivation Kinetics with Other Nerves

The main features of inactivation in the crayfish axon are like those in squid and frog nerves. The steep voltage dependence of the rate of inactivation, particularly in the negative resistance region, and the similar time-courses observed with double- and single-pulse protocols, are in agreement with the results from these preparations (Hodgkin and Huxley, 1952*a*; Chandler et al., 1965; Chiu, 1977; Bezanilla and Armstrong, 1977; Meves, 1977; Gillespie and Meves, 1980; Nonner, 1980). Both of these observations are in contrast to results from the *Myxicola* axon (Goldman and Schauf, 1973; Goldman, 1976; Bullock and Schauf, 1978).

Despite the overall similarity, there are obvious quantitative and qualitative differences from inactivation in squid and frog nerves. The complete decay of sodium currents positive to −40 mV is in contrast to the incomplete fast inactivation seen at all membrane potentials in the squid axon (Chandler and Meves, 1970; Bezanilla and Armstrong, 1977; Meves, 1977; Shoukimas and French, 1980). The single exponential decay of sodium conductance at most membrane potentials is in contrast to the bi-exponential decay observed in the frog node (Chiu, 1977; Nonner, 1980). Quantitatively, inactivation is faster for large depolarizations in crayfish than in squid or frog, and is slower for small depolarizations.

Lag in Inactivation

Delays in double-pulse or prepulse inactivation have previously been reported in *Dosidicus giga* and *Loligo pealei* squid axons (Armstrong, 1970; Bezanilla and Armstrong, 1977; Shoukimas, 1977), *Myxicola* axons (Goldman and Schauf, 1972; Schauf and Davis, 1975), and frog nerve (Peganov, 1973). Some of these results may be subject to the criticisms of Gillespie and Meves (1980). It seems reasonably certain, however, that the lags in inactivation reported here were not caused by insufficient recovery intervals or by series resistance artifacts. This makes it seem very unlikely that the results in the other preparations were entirely artifactual. In the case of *L. pealei,* a delay in inactivation was also observed by comparing currents before and after the removal of inactivation by Pronase (Bezanilla and Armstrong, 1977).

Only small lags have been seen in *Loligo forbesi* axons (Chandler et al., 1965; Gillespie and Meves, 1980) with double-pulse protocols like those used here. The reason for the difference is

not clear. One possibility is that it is due to different experimental conditions: the double-pulse experiments reported here were performed from holding potentials near −80 mV, where inactivation is almost completely removed (Fig. 9), while those of Chandler et al. and Gillespie and Meves began from potentials near −60mV, near the midpoint of the inactivation curve (Chandler et al., 1965); Bezanilla and Armstrong (1977) have reported that a preceding hyperpolarization accentuates the lag in *L. pealei* axons. Another possibility is that the difference reflects a genuine difference in the properties of sodium channels in the two axons. Even if the kinetic pathways for activation and inactivation were basically similar, the more pronounced lag in crayfish axons could arise from quantitative differences in rate constants as compared with those of squid axons. In fact, comparison of inactivation rates at various membrane potentials seems consistent with this explanation. If activation and inactivation are interdependent processes, the lag in double-pulse inactivation would arise from resting or intermediate states inactivating more slowly than open channels. In the crayfish axon, inactivation at −70 mV is slower (time constant ~70 ms. 3°C) than in squid axons (time constant ~20 ms, 0°C; Chandler et al., 1965), as if resting channels inactivate more slowly in crayfish than in squid; on the other hand, inactivation for large depolarizations, where most channels have opened, is faster in crayfish (time constant 0.4–0.6 ms, +30 mV, 3°C) than in perfused squid axons (time constant ~2 ms, +30 mV, 2.4°C; Meves, 1977), as if open channels inactivate more rapidly in crayfish. Whether the difference in time-course of double-pulse inactivation in the two nerves can be explained completely by simply quantitative differences in rate constants will, of course, depend on the precise kinetic scheme for inactivation and on the voltage dependence of the rate constants.

Kinetic Models for the Sodium Channel

It seems premature to propose a specific kinetic model for the sodium channel based on the crayfish axon data, since the kinetics of the activation process have not yet been described in detail. The complexity of the activation kinetics may be illustrated by noting that fitting the complete time-course of the sodium conductance at −15 mV with a sum of exponential terms (Provencher, 1976) required five exponentials; that is, four terms for the activation portion of the curve, in addition to the term corresponding to the decay time constant. The inactivation data alone, however, are enough to suggest likely features of successful sodium channel models.

The principal result is that inactivation becomes faster while channels are activated, but that it is not strictly necessary for channels to open before inactivating. This result is compatible with many specific types of models. For example, it might be that only a few intermediate and open states can inactivate, and that the rate is the same for each; an example of a model of this type is that proposed by Armstrong and Gilly (1979). Alternatively, there could be a gradation of rates of inactivation as channels progress from resting to intermediate to open states; a model of this type has been formulated by Nonner (1980) to fit sodium current and gating charge experiments in frog node.

It should be noted that the results do not necessarily imply a causal link between activation and the rate of inactivation. It is, however, tempting to believe that the relationship is causal. In addition to any steric effects of channel activation, the local electric field must be greatly altered by the movement of the gating charge. If the inactivation process has intrinsic voltage

dependence, as suggested by the data from 0 to +80 mV in Fig. 12, the change in electric field alone could significantly increase the rate of inactivation.

A physical model for inactivation that is in current favor pictures inactivation taking place when open channels are blocked by a positively charged particle that is part of the sodium channel (Armstrong and Bezanilla, 1977). This mechanism has received support from the observation that when inactivation is enzymatically removed, blocking by certain internal cations mimics some aspects of normal inactivation (Yeh and Narahashi, 1978; Eaton et al., 1978; Cahalan and Almers, 1979; Yeh and Armstrong, 1978). The results reported here are inconsistent with the simplest kinetic analogs of such a physical model, which would involve strict coupling of inactivation to the opening of channels. The results would, however, be consistent with versions in which the inner mouth of the channel could be plugged by the inactivating particle before the entire channel had become conducting. This possibility is included in Armstrong and Bezanilla's model (1977), which is therefore at least qualitatively consistent with the present results. It would be interesting to perform experiments like that in Fig. 11 in axons with artificial inactivation induced by internal blocking cations, in order to see if it is strictly necessary for the channels to open before being blocked by these particles.

This work was performed in the laboratory of Dr. Peter Shrager in the Department of Physiology. I am very grateful to him, Dr. Ted Begenisich, and Dr. David Goldstein for encouragement and discussion during this work, and to Dr. R. W. Tsien for comments on a manuscript. A report of the work was submitted to the University of Rochester in 1979 in partial fulfillment of the requirements for the degree of Doctor of Philosophy in Biophysics.

This work was supported primarily by National Institutes of Health grant 5-R01-NS10500 to Dr. P. Shrager and performed in part under contract DE-AC02-76EV03490 with the U. S. Department of Energy at the University of Rochester Department of Radiation Biology and Biophysics and has been assigned report no. UR-3490-1872.

Received for publication 23 July 1980 and in revised form 5 May 1981.

REFERENCES

Armstrong, C. M. 1970. Comparison of *gk* inactivation caused by quaternary ammonium ion with g_{Na} inactivation. *Biophys. J.* 10:185*a*.

Armstrong, C. M., and F. Bezanilla. 1977. Inactivation of the sodium channel. II. Gating current experiments. *J. Gen. Physiol.* 70:567–590.

Armstrong, C. M., and W. F. Gilly. 1979. Fast and slow steps in the activation of sodium channels. *J. Gen. Physiol.* 74:691–711.

Bezanilla, F., and C. M. Armstrong. 1977. Inactivation of the sodium channel. I. Sodium current experiments. *J. Gen. Physiol.* 70:549–566.

Bullock, J. O., and C. L. Schauf. 1978. Combined voltage-clamp and dialysis of *Myxicola* axons: behaviour of membrane asymmetry currents. *J. Physiol. (Lond.).* 278:309–324.

Cahalan, M. D., and W. Almers. 1979. Block of sodium conductance and gating current in squid giant axons poisoned with quaternary strychnine. *Biophys. J.* 27:57–74.

Chandler, W. K., A. L. Hodgkin, and H. Meves. 1965. The effect of changing the internal solution on sodium inactivation and related phenomena in giant axons. *J. Physiol. (Lond.).* 180:821–825.

Chandler, W. K., and H. Meves. 1965. Voltage clamp experiments on internally perfused giant axons. *J. Physiol. (Lond.).* 180:788–820

Chandler, W. K., and H. Meves. 1970. Rate constants associated with changes in sodium conductance in axons perfused with sodium fluoride. *J. Physiol. (Lond.).* 211:679–705.

Chiu, S. Y. 1977. Inactivation of sodium channels: second order kinetics in myelinated nerve. *J. Physiol. (Lond.).* 273:573–596.

Cole, K. S. 1968. Membranes, Ions and Impulses. University of California Press, Berkeley.

Cole, K. S., and J. W. Moore. 1960. Ionic current measurements in the squid giant axon. *J. Gen. Physiol.* 44:123–167.

Eaton, D. C., M. S. Brodwick, G. S. Oxford, and B. Rudy. 1978. Arginine-specific reagents remove sodium channel inactivation. *Nature (Lond.)*. 271:473–476.

Gillespie, J. I., and H. Meves. 1980. The time course of sodium inactivation in squid giant axons. *J. Physiol. (Lond.)*. 299:289–307.

Goldman, L. 1975. Quantitative description of the sodium conductance of the giant axon of *Myxicola* in terms of generalized second order variable. *Biophys. J.* 15:119–136.

Goldman, L. 1976. Kinetics of channel gating in excitable membranes. *Q. Rev. Biophys.* 9:491–525.

Goldman, L., and C. L. Schauf. 1972. Inactivation of the sodium current in *Myxicola* giant axons. Evidence for coupling to the activation process. *J. Gen. Physiol.* 59:659–675.

Goldman, L., and C. L. Schauf. 1973. Quantitative description of sodium and potassium currents and computed action potentials in *Myxicola* giant axons. *J. Gen. Physiol.* 61:361–384.

Hogdkin, A. L., and A. F. Huxley. 1952a. The dual effect of membrane potential on sodium conductance in the giant axon of *Loligo*. *J. Physiol. (Lond.)*. 116:497–506.

Hodgkin, A. L., and A. F. Huxley. 1952b. A quantitative description of membrane current and its application to conduction and excitation in nerve. *J. Physiol. (Lond.)*. 117:500–544.

Hodgkin, A. L., A. F. Huxley, and B. Katz. 1952. Measurement of current-voltage relations in the membrane of the giant axon of *Loligo*. *J. Physiol. (Lond.)*. 116:424–448.

Hoyt, R. C. 1968. Sodium inactivation in nerve fibers. *Biophys. J.* 8:1074–1097.

Hoyt, R. C., and W. J. Adelman, Jr. 1970. Sodium inactivation. Experimental test of two models. *Biophys. J.* 10:610–617.

Jakobsson, E. 1976. An assessment of a coupled three-state model for sodium conductance changes. *Biophys. J.* 16:291–301.

Kniffki, K. D., D. Siemen, and W. Vogel. 1978. Delayed development of sodium permeability inactivation in the nodal membrane. *J. Physiol. (Lond.)*. 284:92–93p. (Abstr.)

Meves, H. 1977. Inactivation of the sodium permeability in squid giant nerve fibres. *Prog. Biophys. Mol. Biol.* 33:207–230.

Meves, H., and W. Vogel. 1977. Inactivation of the asymmetrical displacement current in giant axon of *Loligo forbesi*. *J. Physiol (Lond.)*. 267:377–393.

Nonner, W. 1980. Relations between the inactivation of sodium channels and the immobilization of gating charge in frog myelinated nerve. *J. Physiol. (Lond.)*. 299:573–603.

Oxford, G. S., and J. P. Pooler. 1975. Selective modification of sodium channel gating in lobster axons by 2,4,6-trinitrophenol. Evidence for two inactivation mechanisms. *J. Gen. Physiol.* 66:765–779.

Peganov, E. M. 1973. Kinetics of the process of inactivation of sodium channels in the node of Ranvier of frogs. *Bull. Eksp Biol. Med.* 11:5–9.

Provencher, S. W. 1976. A Fourier method for the analysis of exponential decay curves. *Biophys. J.* 16:27–41.

Schauf, C. L., and F. A. Davis. 1975. Further studies of activation-inactivation coupling in Myxicola axons. Insensitivity to changes in calcium concentration. *Biophys. J.* 15:1111–1116.

Schauf, C. L., T. L. Pencek, and F. A. Davis. 1976. Activation-inactivation coupling in *Myxicola* giant axons injected with tetraethylammonium. *Biophys. J.* 16:985–989.

Shoukimas, J. J. 1977. Effect of calcium upon sodium inactivation in the giant axon of *Loligo pealei*. *J. Membr. Biol.* 38:271–289.

Shoukimas, J. J., and R. J. French. 1980. Incomplete inactivation of sodium currents in nonperfused squid axon. *Biophys. J.* 32:857–862.

Shrager, P. 1974. Ionic conductance changes in voltage-clamped crayfish axons at low pH. *J. Gen. Physiol.* 64:666–690.

Sigworth, F. 1979. Analysis of nonstationary sodium current fluctuations in frog myelinated nerve. Ph.D. Thesis, Yale University.

Swenson, R. P., Jr. 1980. Gating charge immobilization and sodium current inactivation in internally perfused crayfish axons. *Nature (Lond.)*. 287:644–645.

Taylor, R. E., J. W. Moore, and K. S. Cole. 1960. Squid axon voltage clamp measurements. *Biophys. J.* 1:161–202.

Van Harreveld, A. 1936. A physiological solution for freshwater crustaceans. *Proc. Soc. Exp. Biol. Med.* 34:428–432.

Yeh, J. Z., G. S. Oxford, C. H. Wu, and T. Narahashi. 1976. Interactions of aminopyridines with potassium channels of squid axon membranes. *Biophys. J.* 16:77–81.

Yeh, J. Z., and C. M. Armstrong. 1978. Immobilization of gating charge by a substance that stimulates inactivation. *Nature (Lond.)*. 273:387–389.

Yeh, J. Z., and T. Narahashi. 1977. Kinetic analysis of pancuronium interaction with sodium channels in squid axon membranes. *J. Gen. Physiol.* 69:293–323.